



**National Conference on
Advances in Mechanical Engineering and Nanotechnology (AMENT2018)
29-30 June, 2018
Organized by
Department of Mechanical Engineering, University College of Engineering (A),
Osmania University, Hyderabad, TS, India**

Comparative Study of Structured and Unstructured Meshing of Nozzle Model

V. Uma Maheshwar

Department of Mechanical Engineering
University College of Engineering (A),
Osmania University
Hyderabad (T.S.) [INDIA]
Email: mahesh.v@uceou.edu

Moogi Srinivasa Rao

Department of Mechanical Engineering
University College of Engineering (A),
Osmania University
Hyderabad (T.S.) [INDIA]
Email: moogi_75@yahoo.co.in

ABSTRACT

Nozzle is an important component of a missile, rocket or air breathing engine etc., They produce thrust, converting the pressure of the hot chamber gases into kinetic energy and directing that energy along the nozzle axis. Solid rocket motors are used for generation of thrust during launching of aerospace vehicles or missiles. A nozzle is the component of a missile that produces required thrust from hot gases at high pressure to kinetic energy. Depending on the requirement of exit Mach number a suitable nozzle is designed. Convergent – Divergent nozzle is employed for supersonic flows. The paper aims to validate its design and evaluate its ballistic performance. The computational data obtained is validated with experimental data.

The nozzle considered for analysis in the paper is designed for solid Rocket motor of a missile and is made of low alloy steel 15CDV6. Nozzle is modeled in CREO 3.0 and

analysis is carried out in ANSYS 15.0 (ICEMCFD) and simulation is carried in fluent. Comparative study of structured meshing with hexahedral cell and unstructured meshing for convergent – divergent nozzle of missile is presented. The study is aimed at comparative study of structured and unstructured meshing of symmetrical configuration like nozzle. A C-D nozzle model is designed and analyzed by Computational Fluid Dynamics (CFD) for various performance parameters like pressure, temperature and Mach number. The boundary conditions are selected based on conditions of gas at the exit of solid rocket motor. From the results, it can be concluded that the structured and unstructured meshing of axisymmetric nozzle are similar and computational results obtained are closer to the experimental data.

Keywords:—Rocket Nozzle, Structured Meshing, CD Nozzle, Supersonic Nozzle

I. INTRODUCTION

The paper presents a comparative study of structured meshing with hexahedral cell and unstructured meshing with tetrahedral cell for convergent –divergent nozzle of missile.

The quality of the computational results depends strongly on the meshing / grid generation in CFD. The meshing results are compared with help of pressure, Mach number, temperature distribution and density at the different section of the nozzle.

The experimental data has been compared with structured and unstructured stimulation data. The nozzle considered for analysis in the paper is designed for solid Rocket motor of a missile and is made of low alloy steel 15CDV6. Nozzle is modeled in CREO 3.0 and analysis is carried out in ANSYS 15.0 (ICEMCFD) and simulation is carried in fluent. Comparative study of structured meshing with hexahedral cell and unstructured meshing for convergent – divergent nozzle of missile is presented.

The study is aimed at comparative study of structured and unstructured meshing of symmetrical configuration like nozzle. A C-D nozzle model is designed and analyzed by Computational Fluid Dynamics (CFD) for various performance parameters like pressure, temperature and Mach number. The boundary conditions are selected based on conditions of gas at the exit of solid rocket motor.

Literature review has revealed that in the community of computational aerodynamics, a great success of unstructured mesh technologies has been witnessed in the past decades due to its automatic and adaptive abilities for complex geometry configurations [1]. Nowadays, many commercial or in-house codes can generate unstructured meshes in a very reliable and computationally efficient manner. Owing to

the rapid advance of parallel mesh generation algorithms, the time cost consumed by the pipeline of unstructured mesh generation can be further reduced to a very low level [2–5]. For instance, the authors have recently implemented a parallel pipeline where the three major steps of unstructured mesh generation (i.e., surface meshing, volume meshing and volume mesh quality improvement) are all parallelised [4,5]. Experiments show that this parallelised pipeline can employ about 100 computer cores to generate a high-quality mesh composed of hundreds of millions of tetrahedral elements in minutes.

II. PROBLEM DESCRIPTION AND SCOPE OF CURRENT WORK

Approximately 65 to 75 % of total vehicle thrust is developed by acceleration of the chamber products to sonic velocity at the nozzle throat; the remainder is developed by expansion cone. The usual objective of nozzle design is to control the expansion in such a manner that range or payload of the total vehicle is maximize within envelope, weight and cost constraints.

The nozzle is thus an integral component of a large system and cannot be optimized independently of that system. Because of interrelationship, nozzle design is an iterative process in which Aerodynamic design, Thermodynamic design and Structural design are done with fabrication considerations.

Aerodynamic design: The gas-contacting surfaces are configured to produce the required performance within limits. The entry, throat, and exit surfaces are sized and configured to provide the desired thrust.

Thermal design: in which thermal liners (materials that form the physical boundary for the exhaust products) and thermal insulators are selected and configured to

maintain the surfaces as closely as practical against effects of erosion and to limit the temperature to acceptable levels. Throat inserts, thermal liners, and insulators are selected and configured to maintain the aerodynamics design. Thermal design / analysis of a solid rocket motor involves identification of thermal environments in different parts of the motor chamber and nozzle, estimation of heating loads, heat transfer to the primary structure, choice of suitable thermal protection materials and detailed thermal analysis including thermal response of insulating materials/ ablatives.

Solid propellants considered are heterogeneous propellants which contain finely powdered aluminum as an ingredient to increase the specific impulse. The combustion products of such propellants form a two phase mixture of gaseous products and aluminum (Al_2O_3) particles which are in liquid form in the motor chamber and in solid form in the divergent nozzle. Thermal environments due to this hot flowing gas- particle combustion products are:

- Convective heating from the flowing hot gases.
- Radiation heating from the absorbing / emitting components of the products of combustion such as CO , CO_2 , H_2O and HCl etc.

Radiation heating from the solid / liquid particles, which essentially consists of Al and Al_2O_3 . Heating due to particle impingement, particularly in the motor aft-end and convergent region. The situation for the rocket motor nozzle is, however, difference. Nozzle wall are exposed to the hot flowing gases throughout the burn duration of the motor. Significant contribution to overall heating in the divergent nozzle is due to particle impingement. In the divergent nozzle, the heat transfer is essentially due to convective

heating with radiation heating from solid Al_2O_3 particle as the second contributing factor. Nozzle liner: a nozzle can be divided into three regions name Entrance cone or convergent The throat region Exit cone or divergent region.

Structural design: in which materials are selected and configured to support the thermal components and to sustain the predicted loads. The basic structure of both external and submerged nozzles is subjected to internal pressure loads and flight loads.

The internal pressure load is divided into an axial ejection (blowout) load and an opposing axial thrust load; the flight loads include aerodynamic loads, inertial loads, and vibration loads. The governing design requirement generally will fall into one or more of the following four categories.

Strength limitations – the configuration is determined by the ability of the component to withstand the imposed stresses without exceeding the material design strength.

Deflection limitations –the configuration is designed to limit a particular displacement to a predetermined critical value in order to limit strain in the liner and insulator components supported by the structure.

Stability limitations – the configuration is designed to prevent buckling. Economic limitations

Design of nozzle hardware: the convergent part of the nozzle is designed as a pressure vessel, similarly to the dished ends. The pressure intensity in the divergent nozzle gradually reduces and hence the stresses due to the pressure distribution are not significant.

Problems in nozzle design: graphite cracking and ejection, differential erosion at material interfaces, lack of sufficient proven nondestructive testing techniques

(NDT), the uncertainty of adhesive bonding and inadequate definition of material properties, particularly at high temperature.

Two basic nozzle configurations possible is the external nozzle is the classical convergent – divergent or de-Laval nozzle or the submerged – nozzle configuration.

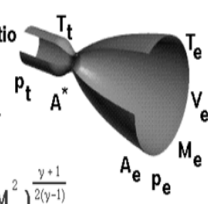
III. METHODOLOGY

The Inlet boundary conditions are taken as given below:

S.No	Parameters	Values
1	Inlet diameter, D_i	258 mm
2	Exit diameter, D_e	147 mm
3	Length of the nozzle	577 mm
4	Throat diameter, D^*	50 mm
5	Exit pressure, p_e	2.2 kg/cm ²
6	Chamber pressure, p_c	128 kg/cm ²
7	Gamma, γ	1.19
8	Molecular weight	28
9	Gas density, ρ	1.86 kg/m ³
10	Viscosity, μ	9.51×10 ⁻⁵ N m/s ²
11	Chamber temperature	320° K

Basic equation of nozzles used are listed as below:

Known:
 p_t = Total Pressure γ = Specific Heat Ratio
 T_t = Total Temperature R = Gas Constant
 p_0 = Free Stream Pressure A = Area



Mass Flow Rate: $\dot{m} = \frac{A^* p_t}{\sqrt{T_t}} \sqrt{\frac{\gamma}{R}} \left(\frac{\gamma+1}{2}\right)^{-\frac{\gamma+1}{2(\gamma-1)}}$

Exit Mach: $\frac{A_e}{A^*} = \left(\frac{\gamma+1}{2}\right)^{\frac{\gamma+1}{2(\gamma-1)}} \left(1 + \frac{\gamma-1}{2} M_e^2\right)^{\frac{\gamma+1}{2(\gamma-1)}}$

Exit Temperature: $\frac{T_e}{T_t} = \left(1 + \frac{\gamma-1}{2} M_e^2\right)^{-1}$

Exit Pressure: $\frac{p_e}{p_t} = \left(1 + \frac{\gamma-1}{2} M_e^2\right)^{-\frac{\gamma}{\gamma-1}}$

Exit Velocity: $V_e = M_e \sqrt{\gamma R T_e}$

Thrust: $F = \dot{m} V_e + (p_e - p_0) A_e$

IV. CALCULATIONS

Average thrust = 3.7 ton
 =3700 kgf
 Total impulse = Thrust × Burning time
 = 3700 × 10
 =37000 kgf-sec

Mass of the propellant = Total Impulse(I_t) / Specific Impulse (I_{sp})

= 37000/240 [Specific Impulse (I_{sp}) =240 to 250 sec]

$m = 154.2$ kg

Mass flow rate (\dot{m}) = 154.2/10

=15.42 kg/ sec

$$(\dot{m}) = \frac{P_c \times A_t}{c^*}$$

Mass flow rate

15.42 = $P_c \times \pi \times D_t^2 \times 9.81 / 4 \times 1600$

[Characteristic Velocity (c^*) = 1520 to 1620 m/s]

$P_c D_t^2 = 15.42 \times 4 \times 1600 / 9.81 \times \pi$

= 3203.8

Table No. 1 : Calculated Values of Chamber Pressure for given Throat Diameter

Chamber pressure (P_c , kg / cm ²)	98	108	118	128	138
Throat diameter (D_t , mm)	57.17	54.46	52.10	50.02	48.18

Area ratio (ϵ)= A_e / A_t [Area ratio (ϵ) = 6 to 10]

8.6 = A_e / A_t

$A_e = 8.6 \times \frac{\pi}{4} \times (50)^2$

$$D_e = 146.6 \approx 147 \text{ mm}$$

At throat of the nozzle

- $$\frac{T_c}{T_t} = 1 + \frac{(\gamma-1)}{2} M_t^2$$

where $M_t = 1$

$$\frac{T_c}{T_t} = \frac{1+(0.19)}{2}$$

where $r=1.19; T_c = 3200\text{K}$
 $T_t \sim 2922 \text{ K}$
- $$\frac{P_t}{P_c} = \left(\frac{2}{r+1}\right)^{\frac{\gamma}{\gamma-1}}$$

where $P_c = 128 \text{ kg/cm}^2$

$$P_t = P_c \times \left(\frac{2}{r+1}\right)^{\frac{\gamma}{\gamma-1}} = 72.5 \text{ kg/cm}^2$$
- $$M = \frac{V_t}{a_t}$$

where $M=1$
 $R = \frac{P_0}{M} = \frac{8314.46}{28} = 296.945 \text{ J/kg mol K}$

$$a_t = \sqrt{rRT_t}$$

$$= \sqrt{(1.19 \times 296.945 \times 2922)}$$

$$= 1016.135 \text{ m/sec}$$

$$1 = \frac{V_t}{a_t}$$

$$V_t = 1016.135 \text{ m/sec}$$

At exit of the nozzle

$$\frac{P_e}{P_t} = \left(1 + \frac{\gamma-1}{2} M_e^2\right)^{-\frac{\gamma}{\gamma-1}}$$

where $M_e = 3.1, \gamma = 1.19$

$$P_e = 2.2 \text{ kg/cm}^2$$

$$\frac{T_e}{T_c} = \left(\frac{P_e}{P_c}\right)^{\frac{\gamma-1}{\gamma}}$$

$$= 3200 \times (2.2/128)^{(1.19-1)/1.19}$$

$$= 1672.8 \approx 1673 \text{ K}$$

$$T_e = T_c \times \left(\frac{P_e}{P_c}\right)^{\frac{\gamma-1}{\gamma}}$$

$$V_e = M_e \sqrt{\gamma RT_e}$$

$$= 3.1 \sqrt{1.19 \times 296.945 \times 1673}$$

$$= 2385.53 \text{ m/s}$$

$$M_e = \frac{V_e}{a_e}$$

$$M_e = \frac{2385.53}{768.88} = 3.10$$

Where $a_e = \sqrt{(\gamma RT_e)}$

$$= \sqrt{(1.19 \times 296.945 \times 1673)}$$

$$= 768.88 \text{ m/s}$$

V. RESULTS OF COMPUTATIONAL SIMULATION

5.1 Modeling and Simulation for Structured Meshing

5.1.1 Meshing/ Grid Generation

Figures 5.1.1, 5.2.1a & b shows Structured Mesh and Unstructured Meshes for the Nozzle. The final refined mesh is shown after several iterations on the refining of the mesh carried out as a part of grid independent study.

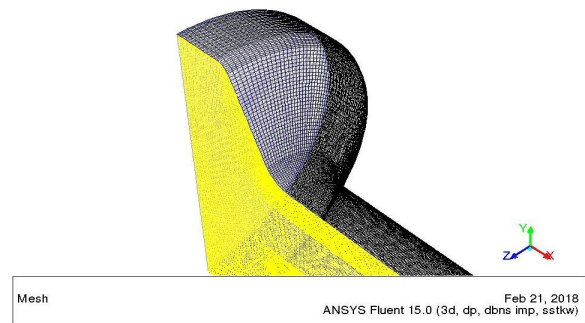


Figure 5.1.1 : Structured Mesh for the Nozzle

5.1.2 Pressure Distribution

Figures 5.1.2 & 5.2.2 shows Pressure contours for Structured Mesh and Unstructured Mesh cases for the Nozzle respectively. The plots clearly show the gradual decrease in the values of pressure typical of a nozzle flow.

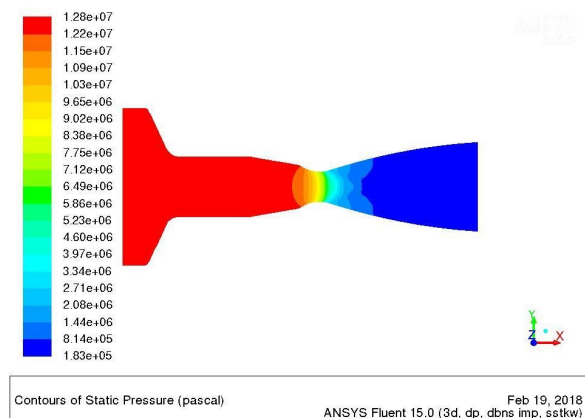


Figure 5.1.2: Static Pressure Contours for Structured Mesh Case

5.1.3 Pressure Varies Along the Nozzle Length

Figures 5.1.3 & 5.2.3 shows Pressure variations along the nozzle length for Structured Mesh and Unstructured Mesh cases for the Nozzle respectively. The plots clearly show the gradual decrease in the values of pressure typical of a nozzle flow.

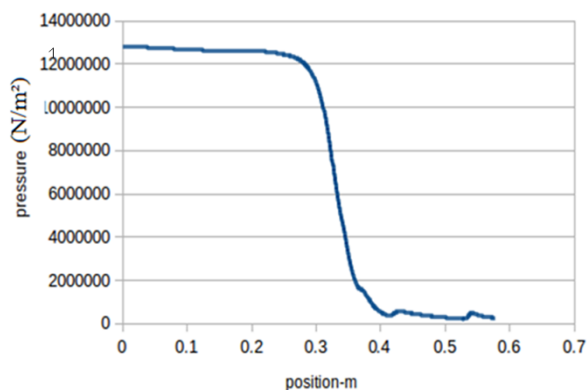


Figure 5.1.3: Pressure variation along the Length of the Nozzle for Structured Mesh Case

5.1.4 Temperature Variation

Figures 5.1.4 & 5.2.4 shows Temperature contours for Structured Mesh and Unstructured Mesh cases for the Nozzle respectively. The plots clearly show the gradual decrease in the values of temperature typical of a nozzle flow.

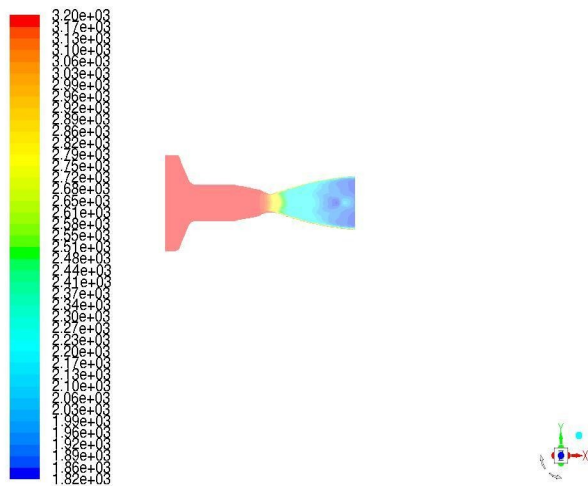


Figure 5.1.4: Temperature Contours for Structured Mesh Case

5.1.5 Temperature Variations along the Nozzle Length

Figures 5.1.5 & 5.2.5 shows Temperature variations along the nozzle length for Structured Mesh and Unstructured Mesh cases for the Nozzle respectively. The plots clearly show the gradual decrease in the values of Temperature typical of a nozzle flow.

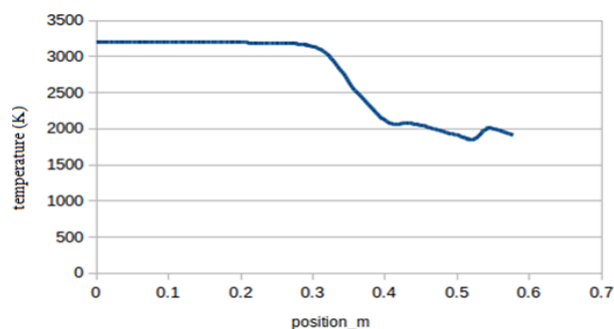


Figure 5.1.5: Temperature variation along the Length of the Nozzle for Structured Mesh Case

5.1.6 Mach Number Variation

Figures 5.1.6 & 5.2.6 shows Mach number contours for Structured Mesh and Unstructured Mesh cases for the Nozzle respectively. The plots clearly shows gradual increase in the values of Mach Number typical of a nozzle from inlet to the outlet. It is due to increase of kinetic energy of the flow along the direction of flow. The flow becomes supersonic at the exit.

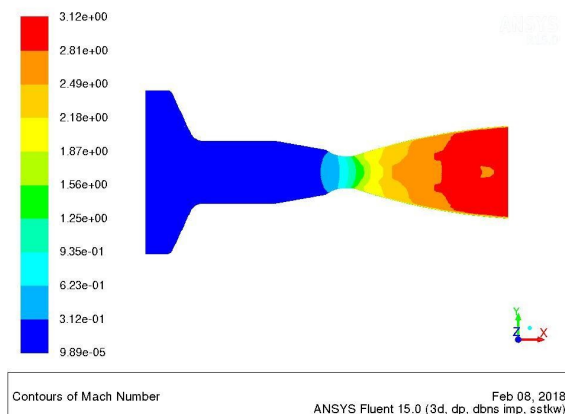


Figure 5.1.6: Mach No. Contour plot for the Nozzle for Structured Mesh Case

5.1.7 Mach number Varies Along With the Length of Nozzle

Figures 5.1.7 & 5.2.7 shows Mach number variation along the length of the nozzle for Structured Mesh and Unstructured Mesh cases for the Nozzle respectively. The plots clearly shows gradual increase in the value s of Mach Number typical of a nozzle from inlet to the outlet. It is due to increase of kinetic energy of the flow along the direction of flow. The flow becomes supersonic at the exit.

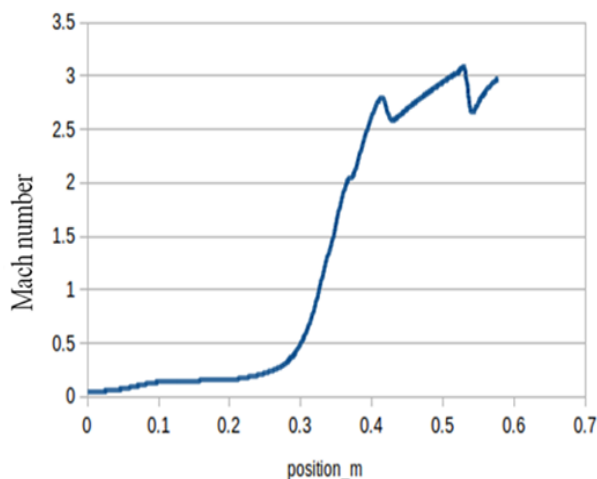


Figure 5.1.7: Mach No. Variation along the Length of the Nozzle for Structured Mesh Case

5.2 Modeling and Simulation for Unstructured Meshing

5.2.1 Unstructured Meshing/ Grid

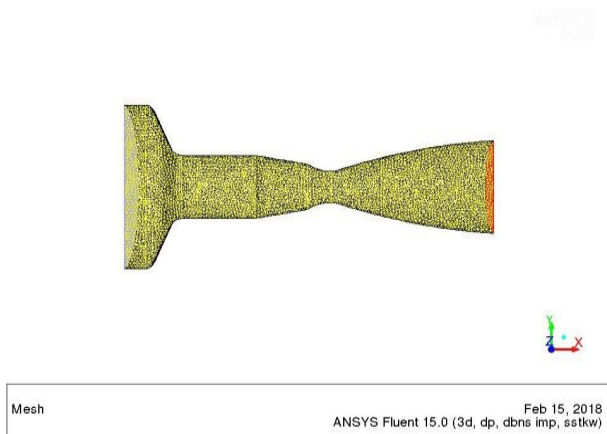


Figure 5.2.1a: Unstructured Mesh for the full length of the Nozzle

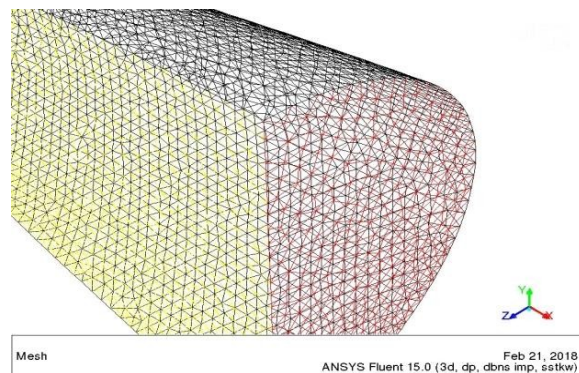


Figure 5.2.1b: Unstructured Mesh for the Nozzle : A close view

5.2.2 Pressure Distribution

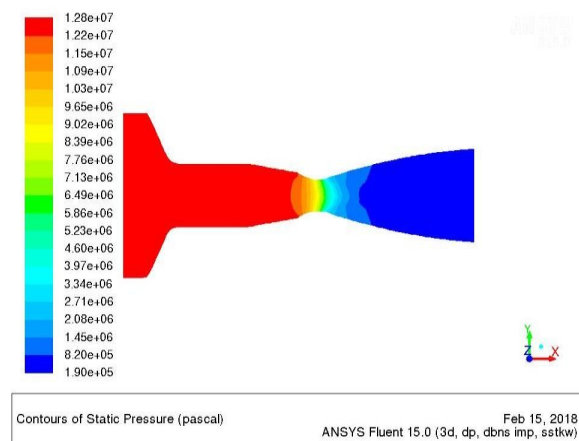


Figure 5.2.2: Static Pressure Contours for Unstructured Mesh Case

5.2.3 Pressure Variation along the Nozzle Length

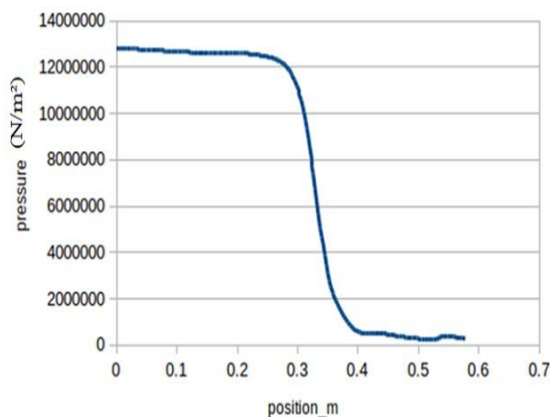


Figure 5.2.3: Pressure variation along the Length of the Nozzle for Unstructured Mesh Case

5.2.4 Temperature Contours

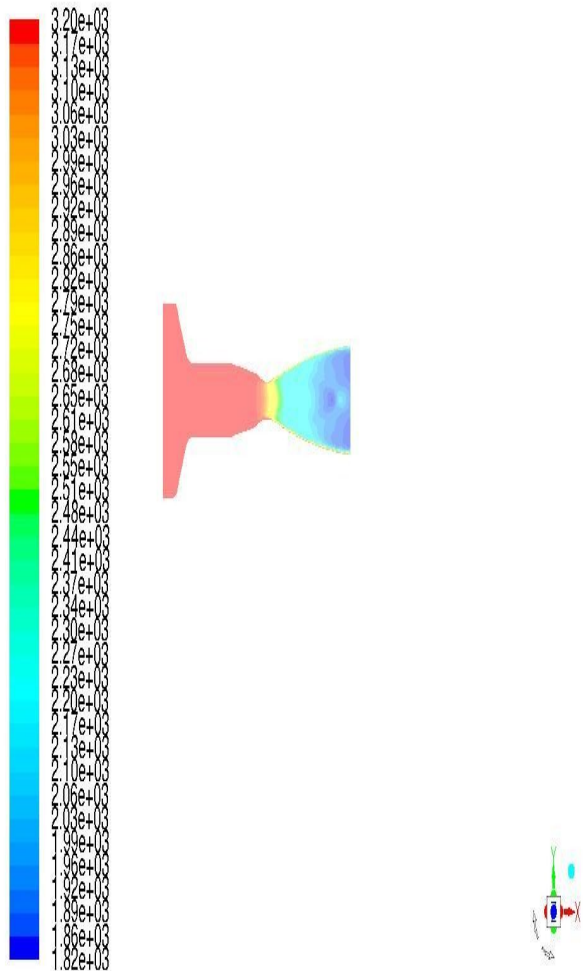


Figure 5.2.4: Temperature Contours for Unstructured Mesh Case

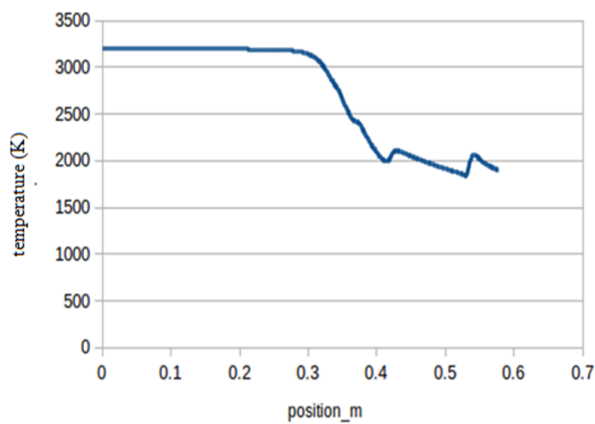


Figure 5.2.5: Temperature variation along the Length of the Nozzle for Unstructured Mesh Case

5.2.6 Mach number Variation

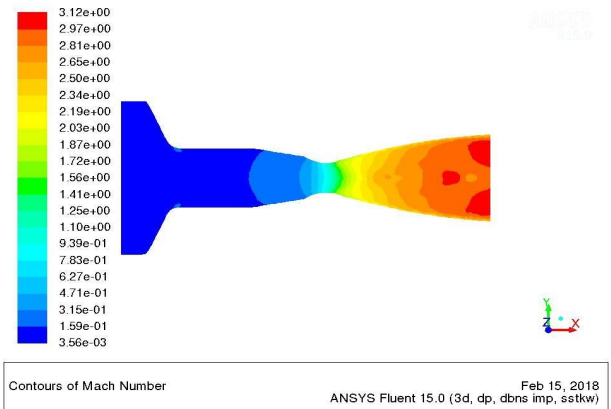
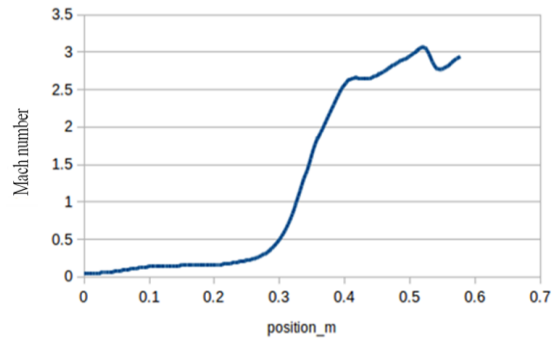


Figure 5.2.6: Mach No. Contour plot for the Nozzle for Unstructured Mesh Case



5.2.7 Mach number Varies Along With the Length of Nozzle

Figure 5.2.7: Mach No. variation along the Length of the Nozzle for Unstructured Mesh Case

VI. CONCLUSIONS

Comparative study of structured and unstructured meshing of three dimensional nozzle model with experimental data is presented in the Table 2. Comparison of R results of current study with Calculated and experimental values shows that the results are similar in nature for both structured and unstructured meshing in nozzle configuration. This is valid as long as axis ym metric configuration is considered. The unstructured meshed model has shown higher values of properties when compared to the Structures meshed model.

Table 2: Comparison of Results of Current Study with Calculated and Experimental Values

	Experimental values (at exit)	Calculated values (at exit)	Structured meshing values (at exit)	Unstructured meshing values (at exit)
Pressure (P), kg/cm ²	1.67	1.78	1.83	1.9
Temperature (T), oK	1617	1673	1821	1824
Mach number (M)	3.01	3.10	3.12	3.12

REFERENCES:

[1] T. J. Baker, Mesh generation: Art or science?, Progress in Aerospace Sciences 41 (2005) 29 – 63.

[2] N. Weatherill, O. Hassan, K. Morgan, J. Jones, B. Larwood, K. Sorenson, Aerospace simulations on parallel computers using unstructured grids, International Journal for Numerical Methods in Fluids 40 (2002) 171–187.

[3] R. Löhner, A 2nd generation parallel advancing front grid generator, in: Proceedings of the 21st International Meshing Roundtable, 2013, pp. 457–474.

[4] J. Chen, D. Zhao, Z. Huang, Y. Zheng, D. Wang, Improvements in the reliability and element quality of parallel tetrahedral mesh generation, International Journal for Numerical Methods in Engineering 92 (2012) 671 –693.

[5] J. Chen, D. Zhao, Y. Zheng, Z. Huang, J. Zheng, Fine-grained parallel algorithm for unstructured surface mesh generation, in:

Proceedings of the 22nd International Meshing Roundtable, 2014, pp. 559 – 578.

[6] Bharath Kumar Komarabathini, Deekshitha Kancharla, Kumari Monika, Praveen Kumar Chikoti and Krupakar Pasala, “Study of Rate of Convergence of different types of Grids in CFD Analysis”, Accepted 10 January 2014, Available online 01 February 2014, Special Issue-2, February 2014.

[7] Steven J. Owen, “A Survey of Unstructured Mesh Generation Technology,” 1998.

[8] E.M. S. Ekanayake, J. A. Gear and Y. Ding, “Numerical Simulation of a Supersonic Convergent Divergent Nozzle with divergent angle variations for Under expanded condition,” 17th Australasian fluid mechanical conference proceedings, 2010.

[9] Zhoufang Xiao, Jianjun Chen, Yao Zheng, Lijuan Zeng, Jianjing Zheng, “Automatic Unstructured Element-Sizing Specification Algorithm for Surface Mesh Generation”, 2014.

[10] Dr.Blazek’s main research interests includes CFD code development especially in the area of unstructured grids, aircraft and turbo machinery aerodynamics, shape optimization and data visualization, 2007.

[11] George P.Sutton, Oscar Biblarz, Rocket propulsion element, John Wiley & Sons, 2017.

[12] C. Hirsch, Numerical Computation of Internal and External Flows. Vol. I and II. John Wiley & Sons, Chichester, 1990.